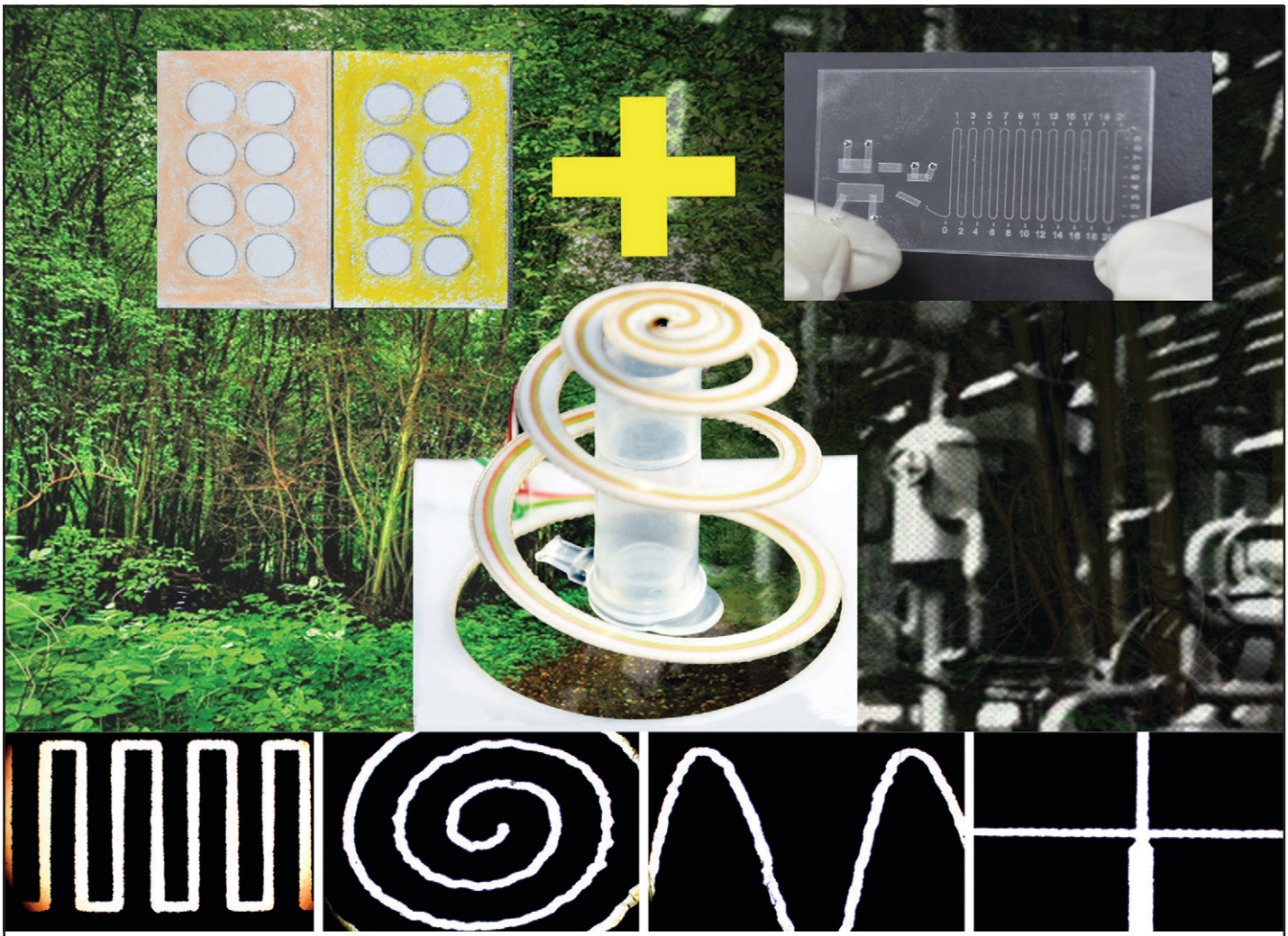

Featuring Work from the Bioinspired Engineering and Biomechanics Center, Prof. Tian Jian Lu and Prof. Feng Xu, Xi'an Jiaotong University, China

Title: Benchtop fabrication of three-dimensional reconfigurable microfluidic devices from paper–polymer composite

A simple and low-cost approach was developed to fabricate three-dimensional reconfigurable microfluidic systems using a paper/polymer composite. The complex microfluidic structures were achieved through bending and stretching.

As featured in:

See Feng Xu *et al.*, *Lab Chip*, 2013, **13**, 4745.

RSC Publishing

www.rsc.org/loc

Registered Charity Number 207890

Lab on a Chip

RSC Publishing

TECHNICAL INNOVATION

View Article Online
View Journal | View Issue

Cite this: *Lab Chip*, 2013, **13**, 4745

Benchtop fabrication of three-dimensional reconfigurable microfluidic devices from paper–polymer composite†

Yu Long Han,[ab] Wenqi Wang,[ab] Jie Hu,[ab] Guoyou Huang,[ab] ShuQi Wang,[c] Won Gu Lee,[d] Tian Jian Lu*[b] and Feng Xu*[ab]

Received 7th August 2013,
Accepted 11th September 2013

DOI: 10.1039/c3lc50919b

www.rsc.org/loc

We presented a benchtop technique that can fabricate reconfigurable, three-dimensional (3D) microfluidic devices made from a soft paper–polymer composite. This fabrication approach can produce microchannels at a minimal width of 100 μm and can be used to prototype 3D microfluidic devices by simple bending and stretching. The entire fabrication process can be finished in 2 hours on a laboratory bench without the need for special equipment involved in lithography. Various functional microfluidic devices (*e.g.*, droplet generator and reconfigurable electronic circuit) were prepared using this paper–polymer hybrid microfluidic system. The developed method can be applied in a wide range of standard applications and emerging technologies such as liquid-phase electronics.

The past decade has witnessed an explosion of microfluidics, where continuous efforts have been made to fabricate complex microfluidic devices from one- (1D) *via* two- (2D) to three-dimensional (3D) ones. Compared with 1D and 2D microfluidic systems, 3D microfluidic devices can offer complex microfluidic paths, and thus significantly expand their capabilities in biomedical applications, such as patterning biomaterials, solving problems in mathematics, mixing solutions in microchannels and mimicking vascular structures.[1–9] More recently, 3D reconfigurable microfluidic devices have shown intriguing advantages in liquid-phase electronics,[10–12] such as mechanically tunable antennae[13] and tactile sensors.[14] Due to their widespread applications, there are emerging demands to develop convenient methods to prototype 3D microfluidic devices in a systematic manner.

Several strategies have been developed to fabricate 3D microfluidic systems, such as direct writing and the layer-by-layer stacking method.[15–20] The direct writing method with a femtosecond laser can provide a straightforward and rapid method to fabricate high-precision 3D microfluidic channels within a glass, which however relies on special instruments (*e.g.*, femtosecond laser).[19] The layer-by-layer stacking approach is the most flexible and robust method that involves alignment and stacking of 2D microfluidic layers into a multi-layered structure.[15] Although this method has a broad topographical generality, the fabrication process is time-consuming and tedious when 3D microfluidic devices have complicated shapes and geometries or they require many layers for active mass transport in a spatially and temporally controlled manner.[21] Therefore, there is still an unmet need for an easy, robust and low-cost way of fabricating 3D microfluidic systems.

More recently, Whitesides *et al.* pioneered in developing open channel microfluidic paper-based analytical devices (μPADs),[22] where liquid flow is driven by pressure instead of capillary force as in conventional μPADs. This addresses the disadvantages associated with conventional μPADs, including limited channel widths, low reagent usage efficiency and incompatibility with multiphase flows such as droplet generation. However, the paper used in μPADs needs to be chemically modified using fluoroalkyl trichlorosilanes in the gas phase, which is complicated due to extra chemical reactions limiting its wide accessibility. Here, we present a new concept of paper–polymer hybrid microfluidics by using commercially available printing paper as a scaffold and a polymer (*e.g.*, polydimethylsiloxane, PDMS) as an impermeable barrier. The bendable property of the paper–polymer composite allows the production of paper–polymer hybrid microfluidics with a unique reconfigurable capability. We demonstrated this rapid prototyping method in fabricating both 3D microfluidics and reconfigurable electronics. This paper–polymer microfluidics significantly facilitates the application of paper in 3D microfluidics at low cost by avoiding the use of expensive

[a] *The Key Laboratory of Biomedical Information Engineering of Ministry of Education, School of Life Science and Technology, Xi'an Jiaotong University, Xi'an, 710049, China. E-mail: fengxu@mail.xjtu.edu.cn*
[b] *Bioinspired Engineering and Biomechanics Center (BEBC), Xi'an Jiaotong University, Xi'an, 710049, China. E-mail: tjlu@mail.xjtu.edu.cn*
[c] *Brigham and Women's Hospital, Harvard Medical School, Boston, MA, USA*
[d] *Department of Mechanical Engineering, College of Engineering, Kyung Hee University, Yongin 446-701, Republic of Korea*

† Electronic supplementary information (ESI) available: Details of experimental procedures as well as supplementary results. See DOI: 10.1039/c3lc50919b

facilities associated with lithography, thus holding great potential to impact multiple research areas such as electronics and biomedicine.

Fabrication of paper–polymer hybrid microfluidic devices

To fabricate a paper–polymer hybrid microfluidic device, the cutter design of a microchannel was drawn and loaded onto a laser program. The laser (Universal VLS2.30, USA) etched a microchannel from double-side adhesive (DSA) tape (8146-2, 3M, USA) that was adhered onto printing paper (80 g, Linghang A4 printing paper, China) (Fig. 1(1)–(2)). Alternatively, the etching process was achieved manually using a knife where appropriate. Next, another protective layer of the DSA tape was carefully removed using tweezers, revealing the bottom adhesive surface. Other printing paper was supplied and pressed onto the bottom permanent adhesive surface as a bottom layer (Fig. 1(3)). The whole assembly was then put into a PDMS (Sylgard 184, Dow Corning, USA) bath (the ratio of base to curing agent, 10 : 1) for 30 min at 4 °C (Fig. 1(4)). Next, the assembly was taken out from the PDMS bath, and the extra PDMS on the assembly surface and in the channel was removed manually using paper tissue (napkin). The assembly was then baked at 80 °C for 10 min (Fig. 1(5)). Then, another layer of paper with two ethched holes as the inlet and outlet after PDMS treatment was pressed onto the top of the assembly to form the channel (Fig. 1A(6)). Alternatively, the inlet and outlet holes were etched on transparent DSA tape and directly adhered to the assembly, for the convenience of direct visualization and observation (Fig. 1(6)). Finally, the device was baked at 80 °C for an additional 50 min.

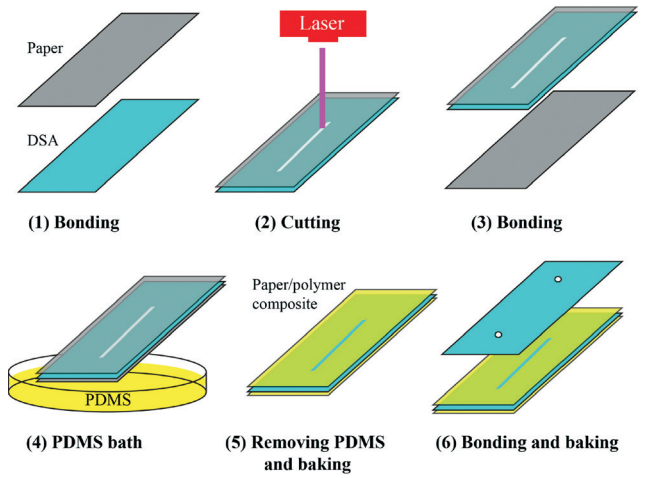

Fig. 1 Schematic illustration of the fabrication process of a hybrid microfluidic channel made from paper and PDMS. (1) Bonding paper and a double side adhesive (DSA) to form a double layer composite. (2) Cutting through this composite to form a hollow channel using a laser machine or knife. (3) Bonding a new layer of paper through DSA to form the bottom of the channel. (4) Immersing the construct in a PDMS bath for 30 min. (5) Removing the redundant PDMS on the surface and within the channel and baking at 80 °C for 10 min. (6) Bonding paper, which has already been immersed in PDMS, on the top of the channel and baking at 80 °C for an additional 50 min. Or the top of the channel can be replaced by a layer of DSA, for the purpose of visualization of the liquid in the channel in the case of opaque paper.

Device examples

To demonstrate the topographical generality of the developed approach in fabricating 2D microchannels, we first fabricated a 2D droplet generator (Fig. 2A). The droplet generator was composed of four 130 μm deep microchannels (*i.e.*, thickness of one layer of paper and DSA tape), among which three are of 300 μm width and the fourth one is of 350 μm width connected with the other three with a 100 μm wide neck.

Fluid flows (one red colored food dye in DI water solution and two transparent mineral oil) were pumped by syringe pumps (TJ-1A and LSP02-1B syringe pump controllers, Longerpump, China) at a flow rate of 10 μL min^{-1} for oil and 2 μL min^{-1} for DI water per inlet (Video 1, ESI†). The droplet can be generated stably, indicating that the paper–polymer microfluidics may serve as an alternative to conventional PDMS based microfluidics.

To demonstrate the versatility of the developed approach in fabricating 3D microchannels, we fabricated a 3D spiral microchannel mixer by stretching a 2D helix microchannel

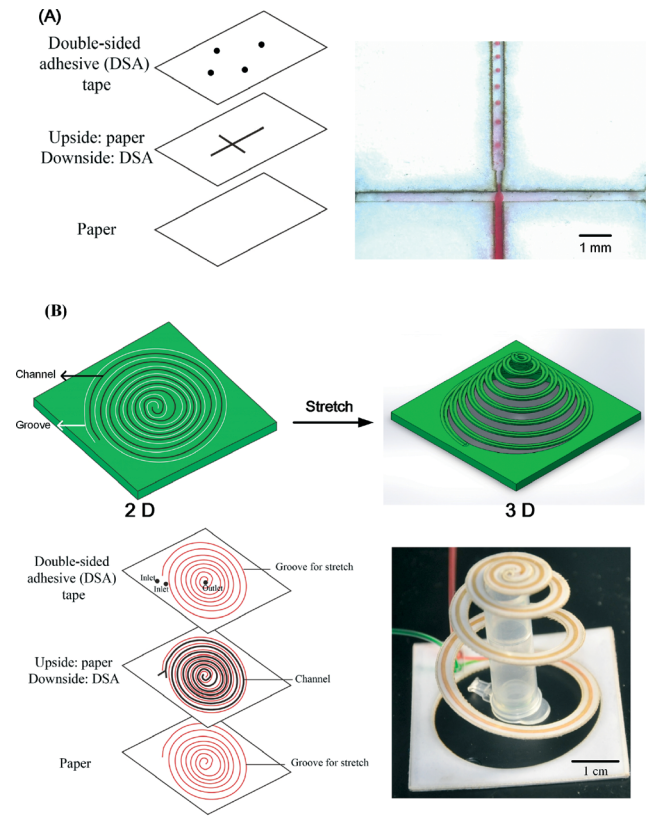

Fig. 2 Representative examples of 2D and 3D hybrid microfluidic structures by benchtop fabrication. (A) A droplet generator with crossed microchannel. Flow rates were 2 μL min^{-1} (red colored food dye) and 10 μL min^{-1} (oil). (B) 3D spiral microchannel mixer was fabricated by upward stretching in an out-of-plane format. The red and green colored food dyes were provided at a flow rate of 2 μL min^{-1}. The microchannel was 700 μm wide and 130 μm deep.

with patterned grooves (Fig. 2B). The microchannel was 700 μm wide and 130 μm deep. The fluid flows (green and red colored food dyes) were injected by syringe pumps at a flow rate of 2 μL min^{-1} per inlet (Video 2, ESI†). The results demonstrate that the stretch did not affect the tightness of the microchannel because two liquids mixed well without any leakage.

Microfluidic channels embedded with liquid metal have drawn increasing interest as electrical wiring or sensors for wearable technologies due to their stretchable and reconfigurable abilities.[14,23–28] To further demonstrate the potential applications of the developed approach for electronics, we built up a liquid electronic circuit system using a straight microchannel (Fig. S1†) embedded with liquid metal (Gallium–Indium Alloys, Sigma) (Fig. 3). Firstly, we made three types of logic gates in the electronic circuit, inducing "OFF", "ON" and "SWITCH" (Fig. 3A). The "OFF" and "ON" were performed by the flow of metal liquid inside the channel, where no liquid flow represented "OFF" and the presence of liquid flow represented "ON", respectively. The "SWITCH" was achieved by the reconfiguration of the microchannel, *i.e.*, mechanically bending the microchannel. Fig. 3B–C depict the electronic circuit built for our experiments. When the liquid metal was pumped into the channel, the blue LED was turned on (Fig. 3D). While mechanically bending the microchannel to the right and left, the green and red LEDs were turned on respectively (Fig. 3D). These results indicate that the hybrid microchannel presented here could have significant impact on reconfigurable electronics, and provide a low-cost choice for wearable technologies.

Fabrication quality and limitation

To check the effect of PDMS infiltration on the structure of porous paper, we used scanning electron microscopy (SEM) to trace the surface roughness (Fig. 4A–B). We observed that the pores on the surface of the paper were physically blocked

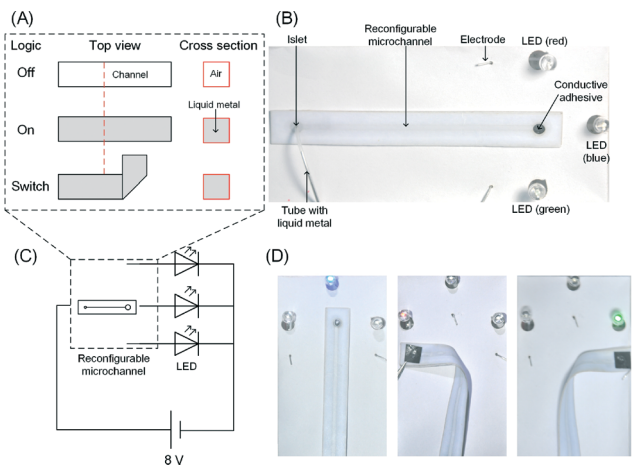

Fig. 3 Hybrid microfluidics as a reconfigurable component in an electronic circuit. (A) Achievement of three types of logic gates in a reconfigurable microchannel with liquid metal, namely "OFF", "ON" and "SWITCH". (B–C) Electronic circuit. (D) Reconfiguration of electronic circuit.

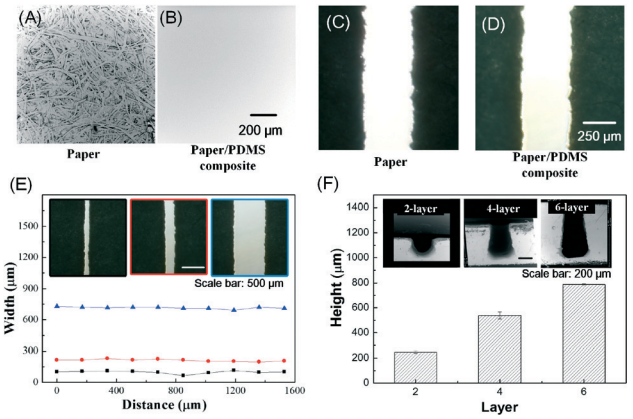

Fig. 4 Fabrication quality and limitation. SEM images of paper (A) before and (B) after PDMS infiltration. Photos of channel (C) before and (D) after PDMS infiltration. (E) Width control of microchannel by laser cutting and variances along the channel. (F) Height control of microchannel by varying layers of paper.

by PDMS after PDMS infiltration and the surface of the paper–polymer hybrid became smooth. Physical blocking makes the paper hydrophobic and thus water impermeable, and the smooth surface may benefit the flow inside the channel. We also quantified the roughness of the paper–polymer hybrid using AFM at a 25 μm^2 area (Fig. S6†), and the roughness (R_a) was 1.86 nm. Compared with R^F Paper[29] (produced by silanization of paper with fluoroalkyl trichlorosilanes) as used in the open channel μPADs, the paper–polymer composite may offer advantages in reducing flow resistance and nonspecific absorption.

To check the effect of PDMS infiltration on the structure of the channel, we measured the changes in the width of the fabricated channel before and after PDMS infiltration (Fig. 4C–D). We further quantified the width changes along the channel (Fig. S2A†) and found that there was no significant difference (Fig. S2B†) (p = 0.40, double side, paired-sample t-test). To test the range of the width that can be fabricated with this method, we manufactured a series of designed channel widths (Fig. 4E). The minimal width was ~90 μm while we envisioned that there is no limitation in the largest width, which covers the scale of commonly used microfluidics (*i.e.*, 200–500 μm), especially for most practical applications. The minimal width was determined by the size of the laser spot (70 μm in diameter) and the ablation of paper. To evaluate the ablation of paper by laser, we tested the effect of laser power on the width of the microchannel by etching a line on one layer of the paper (Fig. S3†). The channel width increased with increasing laser power and the minimal width (88 ± 19 μm) was achieved at 10% power. Power lower than 10% cannot ablate the paper thoroughly and therefore hampers the connectivity of the microchannel. We also observed that the channel wall was not smooth, which was caused by the ablation of the laser. To evaluate this effect, we quantified the changes in the channel width along the channel (Fig. 4E), and no significant variation was observed especially for channels with larger widths. The channel height can also be controlled through regulating the number of stacked paper layers,

which increases linearly with increasing number of layers. For instance, we fabricated channels with 2, 4 and 6 layers, which resulted in channel heights of 249 ± 9 μm, 539 ± 28 μm, 787 ± 8 μm, respectively (Fig. 4F). To evaluate the thickness variation of the microchannel that may be caused by the flowing of PDMS during fabrication, we measured the thickness in the cross section after curing, and no significant variation was observed (Fig. S4†).

All the fabrication procedures were implemented through a benchtop process without the need for any special facilities, such as those involved in photolithography and post-fabrication, leading to a new fabrication process at a simple-step and low-cost level. The potential contamination caused by DSA was avoided by the use of contaminant-free DSA.[30] The cost-effectiveness can be further improved by replacing laser etching with manual cutting (*e.g.*, using a knife) at a reasonable compromise of fabrication accuracy. We have demonstrated this by manually fabricating different patterns of microchannels from a paper–polymer composite (Fig. S7–8†). Compared to pure polymer (such as PDMS), the paper–polymer composite provides a low-cost material to fabricate 3D microchannels that can be stretched and bent.

Conclusion

In this study, we developed an easy and low-cost approach to fabricate reconfigurable microfluidic systems using a paper–PDMS composite that is capable of bending and stretching. We demonstrated the capability of the developed method by fabricating various 2D and 3D microfluidic systems with channel width as small as 100 μm, including a droplet generator, 3D helical mixer and reconfigurable electronic circuit. The whole manufacturing process from device design to working device can be completed in 2 hours on the laboratory bench without using lithography. Although we used PDMS in this study, this approach can be compatible with other polymers. For instance, we can use SU-8 as impermeable barriers in the paper–polymer composite to improve solvent compatibility. Owing to its flexibility and simplicity, we believe that the developed method will not only have significant impact on microfluidic fabrication progress but also encourages innovation in a wide range of application areas.

Acknowledgements

This work was financially supported by the National 111 Project of China (B06024), the Major International Joint Research Program of China (11120101002), the Key (Key grant) Project of Chinese Ministry of Education (313045), South Wisdom Valley Innovative Research Team Program, International Science & Technology Cooperation Program of China (2013DFG02930), the Fundamental Research Funds for the Central Universities, and China Postdoctoral Science Foundation funded project (2013M532054), the National Research Foundation of Korea (NRF-2012029193) and Basic Science Research Program through the NRF, funded by the Ministry of Science, ICT and Future Planning (2013010861). FX was also partially supported by the China Young 1000-Talent Program and Program for New Century Excellent Talents in University (NCET-12-0437).

Notes and references

1 D. T. Chiu, N. L. Jeon, S. Huang, R. S. Kane, C. J. Wargo, I. S. Choi, D. E. Ingber and G. M. Whitesides, *Proc. Natl. Acad. Sci. U. S. A.*, 2000, **97**, 2408–2413.
2 D. T. Chiu, E. Pezzoli, H. Wu, A. D. Stroock and G. M. Whitesides, *Proc. Natl. Acad. Sci. U. S. A.*, 2001, **98**, 2961–2966.
3 A. W. Martinez, S. T. Phillips and G. M. Whitesides, *Proc. Natl. Acad. Sci. U. S. A.*, 2008, **105**, 19606–19611.
4 W. Wu, A. DeConinck and J. A. Lewis, *Adv. Mater.*, 2011, **23**, H178–H183.
5 R. H. Liu, M. A. Stremler, K. V. Sharp, M. G. Olsen, J. G. Santiago, R. J. Adrian, H. Aref and D. J. Beebe, *J. Microelectromech. Syst.*, 2000, **9**, 190–197.
6 A. D. Stroock, S. K. Dertinger, A. Ajdari, I. Mezić, H. A. Stone and G. M. Whitesides, *Science*, 2002, **295**, 647–651.
7 M. A. Burns, B. N. Johnson, S. N. Brahmasandra, K. Handique, J. R. Webster, M. Krishnan, T. S. Sammarco, P. M. Man, D. Jones and D. Heldsinger, *Science*, 1998, **282**, 484–487.
8 M. A. Eddings, J. W. Eckman, C. A. Arana, G. A. Papalia, J. E. Connolly, B. K. Gale and D. G. Myszka, *Anal. Biochem.*, 2009, **385**, 309–313.
9 W. A. Farahat, L. B. Wood, I. K. Zervantonakis, A. Schor, S. Ong, D. Neal, R. D. Kamm and H. H. Asada, *PLoS One*, 2012, **7**, e37333.
10 O. J. Schueller, X.-M. Zhao, G. M. Whitesides, S. P. Smith and M. Prentiss, *Adv. Mater.*, 1999, **11**, 37–41.
11 E. Palleau, S. Reece, S. C. Desai, M. E. Smith and M. D. Dickey, *Adv. Mater.*, 2013, **25**, 1589–1592.
12 R. K. Kramer, C. Majidi and R. J. Wood, *Adv. Funct. Mater.*, 2013, DOI: 10.1002/adfm.201203589.
13 P. Yong-Lae, M. Carmel, K. Rebecca, B. Phillipe and J. W. Robert, *J. Micromech. Microeng.*, 2010, **20**, 125029.
14 R. D. Ponce Wong, J. D. Posner and V. J. Santos, *Sens. Actuators, A*, 2012, **179**, 62–69.
15 M. Zhang, J. Wu, L. Wang, K. Xiao and W. Wen, *Lab Chip*, 2010, **10**, 1199–1203.
16 P. K. Yuen and V. N. Goral, *Lab Chip*, 2010, **10**, 384–387.
17 B. H. Jo, L. M. Van Lerberghe, K. M. Motsegood and D. J. Beebe, *J. Microelectromech. Syst.*, 2000, **9**, 76–81.
18 H. Wu, T. W. Odom, D. T. Chiu and G. M. Whitesides, *J. Am. Chem. Soc.*, 2003, **125**, 554–559.
19 Y. Liao, J. Song, E. Li, Y. Luo, Y. Shen, D. Chen, Y. Cheng, Z. Xu, K. Sugioka and K. Midorikawa, *Lab Chip*, 2012, **12**, 746–749.
20 R. R. Gattass and E. Mazur, *Nat. Photonics*, 2008, **2**, 219–225.
21 C. M. Hwang, W. Y. Sim, S. H. Lee, A. M. Foudeh, H. Bae, S.-H. Lee and A. Khademhosseini, *Biofabrication*, 2010, **2**, 045001.

22 A. C. Glavan, R. V. Martinez, E. J. Maxwell, A. B. Subramaniam, R. M. D. Nunes, S. Soh and G. M. Whitesides, *Lab Chip*, 2013, **13**, 2922–2930.
23 Y.-L. Park, B.-R. Chen and R. J. Wood, *IEEE Sens. J.*, 2012, **12**, 2711–2718.
24 Y.-L. Park, C. Majidi, R. Kramer, P. Bérard and R. J. Wood, *J. Micromech. Microeng.*, 2010, **20**, 125029.
25 C. Majidi, R. Kramer and R. Wood, *Smart Mater. Struct.*, 2011, **20**, 105017.
26 S. Cheng and Z. Wu, *Lab Chip*, 2010, **10**, 3227–3234.
27 J. A. Rogers, T. Someya and Y. Huang, *Science*, 2010, **327**, 1603–1607.
28 D.-H. Kim and J. A. Rogers, *Adv. Mater.*, 2008, **20**, 4887–4892.
29 A. C. Glavan, R. V. Martinez, A. B. Subramaniam, H. J. Yoon, R. M. D. Nunes, H. Lange, M. M. Thuo and G. M. Whitesides, *Adv. Funct. Mater.*, 2013, DOI: 10.1002/adfm.201300780.
30 S. Wang, X. Zhao, I. Khimji, R. Akbas, W. Qiu, D. Edwards, D. W. Cramer, B. Ye and U. Demirci, *Lab Chip*, 2011, **11**, 3411–3418.